

Linear-limit aging times of three monoalcohols

Jan Philipp Gabriel,^{1,2,*} Jeppe C. Dyre,^{1,†} and Tina Hecksher^{1,‡}

¹*Glass and Time, IMFUFA, Department of Science and Environment, Roskilde University, Roskilde, Denmark*

²*Institute of Materials Physics in Space, German Aerospace Center, 51170 Cologne, Germany*

(Dated: February 10, 2025)

This paper presents data for the physical aging of the three monoalcohols 2-ethyl-1-butanol, 5-methyl-2-hexanol, and 1-phenyl-1-propanol. Aging is studied by monitoring how the dielectric loss at a fixed frequency in the kHz range equilibrates upon temperature jumps of a few Kelvin's magnitude from equilibrium to equilibrium. The three alcohols differ in the Debye relaxation strength and how much the Debye relaxation time is different from that of the α process. We first demonstrate that single-parameter aging describes all data well and proceed to use this to identify linear-limit normalized aging relaxation functions. From the Laplace transform of these functions, the linear-limit aging loss-peak angular frequency defines the inverse of the linear aging relaxation time. This allows for a comparison to the temperature dependence of the Debye and α dielectric relaxation times of the three monoalcohols. We conclude that the aging response for 5-methyl-2-hexanol and 2-ethyl-1-butanol follows the α relaxation, not on the Debye process, while no definite conclusion can be reached for 1-phenyl-1-propanol because the Debye and α relaxations are here too merged to be distinguished.

I. INTRODUCTION

Physical aging is a characteristic feature taking place, in principle, in all glasses. It involves rearrangement of molecules below the glass transition temperature T_g , reflecting the fact that any glass continuously approaches the equilibrium liquid state [1, 2]. This can only be observed just below T_g , however, because aging is too slow at lower temperatures – aging of window glass is for instance not an issue. Understanding physical aging to the extent of being able to predict it quantitatively is important for applications of oxide glasses, polymers, metallic glasses, etc., both in production and subsequent use [3–15].

The physical aging induced by a continuously changing temperature, e.g., as experienced during the production of glasses, is more difficult to model quantitatively than aging following a temperature jump. An ideal temperature jump starts from the glass-forming liquid annealed to equilibrium at the initial temperature, T_i , and changes the temperature rapidly to the final (annealing) temperature, T_a , which is kept constant for enough time that the system eventually reaches equilibrium at (we denote the final temperature by T_a and not by T_f , which in aging contexts symbolizes the fictive temperature [7, 16]). The temperature change should be fast enough that virtually no relaxation takes place before the new temperature by heat conduction is established uniformly throughout the sample. After the jump, aging is monitored by measuring how some physical property, $X = X(t)$, approaches its equilibrium value. In the data reported below the property X is the dielectric loss at a fixed frequency in the kHz range, but X can also be, e.g., the density, the enthalpy, the dc conductivity, an elastic modulus, linear or nonlinear dielectric properties, etc [3, 5, 17–27]; aging of the structural relaxation time itself can be determined from strain-rate switching experiments, as recently convincingly demonstrated by Ediger and coworkers [28]. The only requirement is that an accurate measurement of X can be accomplished within a short time window during which the system only changes its properties insignificantly.

Achieving close-to-ideal temperature-induced aging conditions is not trivial, primarily because heat conduction is notoriously slow. We obtain such temperature jumps by working with a thin sample and by quickly changing the temperature utilizing a Peltier element close to the sample [29]. Recent alternative approaches to studies of physical aging include that of Henot *et al.*, who used Ohmic heating to obtain extremely fast heating rates [30], and that of Cangialosi and co-workers utilizing the small sample size in fast scanning calorimetry to perform almost instantaneous temperature jumps [31, 32].

Physical aging is highly nonlinear in the sense that different temperature jumps generally result in quite different normalized relaxation functions $R(t)$ defined by

$$R(t) \equiv \frac{X(t) - X_a}{X_i - X_a}. \quad (1)$$

* jan.gabriel@dlr.de

† dyre@ruc.dk

‡ tihe@ruc.dk

Here X_i and X_a are the equilibrium values of the monitored property at the initial temperature T_i and the final (annealing) temperature T_a , respectively. It is henceforth assumed the jump takes place at $t = 0$. Strong nonlinearity is usually observed even for temperature jumps of just 1% magnitude in the sense that down jumps are much faster and more stretched than up jumps of same magnitude to the same final temperature. This is referred to as the “asymmetry of approach”, with up jumps being “autocatalyzed” and down jumps “autoretarded” [7, 10, 12, 17, 33].

The asymmetry of approach has been understood since long as an effect of the so-called material time, which controls the aging and is characterized by a rate of change that itself ages. The rate of aging of a temperature down jump decreases gradually and converges to the equilibrium aging rate at T_a , whereas for an up jump the aging rate increases from a low value to also eventually approach the T_a equilibrium aging rate. A quantitative formalism has existed since 1971 [3], the so-called Tool-Narayanaswamy (TN) formalism, which accounts well for the nonlinearity of temperature jumps and, in fact, of any temperature protocol. An excellent account of the TN formalism was given by Scherer in his 1986 textbook [7].

We used above the term “equilibrium aging rate”, which may seem like a contradiction in terms. Like any other response property, physical aging has a linear limit. Thus standard linear-response theory characterized by linearity and time-translational invariance applies for sufficiently small temperature jumps. This limit, which is approached only for temperature changes smaller than about 0.1%, corresponds to the situation in which the material time is a linear function of time throughout the aging process. A fluctuation-dissipation theorem exists also for linear physical aging, meaning that the aging response for very small jumps is determined by the *equilibrium fluctuations* [34]. It is in this sense an “equilibrium aging rate” may be defined [35].

The linear limit of physical aging was reached experimentally by Riechers *et al.* [36], who reported data for aging following temperature jumps of varying amplitude, the smallest being just 10 mK [36]. That paper applied a simplified version of the TN formalism, the so-called single-parameter-aging (SPA) formalism from 2015 [37], to predict the results of nonlinear temperature jumps from those of small, linear jumps. Following Ref. 35, we use in this paper SPA to do the opposite: from nonlinear temperature jump data SPA is utilized to extract the difficult-to-measure linear aging relaxation function.

The investigation presented below involves three monoalcohols. Monoalcohols are generally good glass formers, but differ from other organic glass-forming liquids by usually having a Debye process as the slowest and most intense dielectric relaxation process [38]. This is believed to reflect the dynamics of hydrogen-bonded structures, a process that is separate from the ordinary α relaxation associated with structural relaxation [38]. Most other linear-response functions have no – or merely very weak – relaxations at the dielectric Debye loss-peak frequency; they instead relax on more or less the time scale of the “ordinary” α relaxation process [38]. In particular, calorimetric measurements of monoalcohols generally correlate with the α relaxation rather than with the Debye process [39, 40].

The question we address below is how physical aging proceeds in monoalcohols: Does aging take place on the time scale of the α process, as one may expect from the general identification of aging as reflecting structural relaxation [7, 12], or does aging proceed on the time scale of the slower dielectric Debye process? Since α linear responses may differ in their corresponding relaxation time but otherwise have identical temperature dependence [41–44], we focus on comparing the aging relaxation time’s temperature dependence to those of the Debye and α relaxation times. In order to do this, however, it is necessary to have linear-response aging data at disposal, which as mentioned may be obtained from nonlinear aging data utilizing SPA.

The investigation proceeds in two steps. First, we validate that the aging data conform to the SPA framework. This has previously been done for glycerol and for several van der Waals bonded liquids, as well as in computer simulations [35–37, 45–49], but not for monoalcohols that as mentioned have quite distinct properties. Once SPA has been validated, we proceed to use it to address whether physical aging as regards the temperature-dependence of the relaxation time follows the Debye process or the α process. Since the purpose is to compare to the temperature dependence of the dielectric Debye and the α relaxation times defined by $\tau = 1/(2\pi\nu_{max})$ in which ν_{max} is the corresponding loss-peak frequency, we use the same equation to determine the “equilibrium” aging relaxation time τ_R from the loss-peak frequency ν_{max}^R of the frequency response obtained by Laplace transforming the SPA-extracted linear-limit aging relaxation function.

II. METHODS

A. Experimental details

The three monoalcohols studied are: 2-ethyl-1-butanol (“2E1B”; Alfa Aesar, 99 % purity), 5-methyl-2-hexanol (“5M2H”; Sigma Aldrich, 99 % purity), and 1-phenyl-1-propanol (“1P1P”; Alfa Aesar, 98+% purity). All liquids were used as purchased.

We monitored aging after temperature jumps by continuously measuring the dielectric loss by means of a high-resolution Andeen-Hagerling AH2700A bridge. This was done at 1 kHz for 5M2H and at 10 kHz for 2E1B and 1P1P. The dielectric loss is the monitored property $X(t)$ in Eq. (1). Alternatively, one can use for $X(t)$ the real part of the dielectric constant; this gives more noisy data but leads to virtually the same linear aging relaxation times (data not shown). Our aging setup, which allows for accurate temperature control and rapid temperature jumps using a Peltier element and a thin liquid film (50 microns), is described in detail in Ref. 29.

The spectra in Figs. 1 and 2 were measured with an HP 3488A Multimeter in conjunction with a custom-built frequency generator covering 10^{-2} - 10^2 Hz and an HP 4284A LCR meter covering 10^2 - 10^6 Hz.

B. Obtaining the linear-limit aging response function from nonlinear temperature jump data via the single-parameter-aging formalism

The TN formalism assumes the existence of a material time, ξ , with the property that all temperature jumps lead to the same normalized relaxation function $R(t)$ when given in terms of ξ . Thus according to TN, if one writes for any specific temperature jump $R(t) = \phi(\xi(t))$, the function ϕ is the same for all jumps whereas the functional form of $\xi(t)$ depends on the jump (usually strongly). If the jump goes from T_i to $T_a = T_i + \Delta T$ where ΔT is the temperature change, SPA makes the following ansatz for the aging rate γ [37, 50]

$$\gamma(t) \equiv \frac{d\xi}{dt}(t) = \gamma_a e^{-c\Delta TR(t)}. \quad (2)$$

Here γ_a is the equilibrium linear aging rate at the final temperature of the jump, T_a , and c is a material-specific constant. Note that the notation used follows that of Ref. 50 and differs from that of Ref. 37, which followed the old tradition in the aging field of defining ΔT as $T_i - T_a$, not as $T_a - T_i$, and which used a dimensionless version of the material-specific “non-linearity parameter” c . Note also that the material time – and thereby the aging rate γ – is only defined within an arbitrary multiplicative constant.

Refs. 37 and 51 showed how to use SPA to calculate the normalized relaxation function of one nonlinear temperature jump from that of another, Ref. 35 showed how SPA allows for calculating the linear limit of a nonlinear jump, and Ref. 36 showed how SPA can be used for calculating nonlinear jumps from linear ones. Although the reasoning is the same in all cases, we now for completeness summarize how SPA is used for calculating the linear-limit normalized aging relaxation function $R_{\text{lin}}(t)$ from the normalized relaxation function $R(t)$ of a general, nonlinear jump.

For $R_{\text{lin}}(t)$ the expression $R(t) = \phi(\xi(t))$ reduces to $R_{\text{lin}}(t_0) = \phi(\gamma_a t_0)$ because $\xi = \gamma_a t_0$ in equilibrium at T_a as well as very close to T_a (the laboratory time of a linear-limit temperature jump is denoted by t_0 to distinguish it from the laboratory time t of general, nonlinear jumps). Taking the time derivatives leads to $dR/dt = \phi'(\xi(t))\gamma(t)$ and $dR_{\text{lin}}/dt_0 = \phi'(\xi = \gamma_a t_0)\gamma_a$, respectively. The ratio of these two equations evaluated at times t and t_0 corresponding to the same value of R (and thus the same material time ξ) is by Eq. (2) equal to $\exp(-c\Delta TR)$. For the ratio between the change of t and t_0 corresponding to the same changes of R , dR , one thus has

$$\frac{dt_0}{dt} = \frac{dR/dt}{dR/dt_0} = \frac{\gamma(t)}{\gamma_a} = e^{-c\Delta TR}, \quad (3)$$

which means that

$$dt_0 = e^{-b\Delta TR} dt. \quad (4)$$

For a temperature up jump one has $\Delta T > 0$ and the time increment dt needed for a given change of the normalized relaxation function, dR , is larger than the time increment dt_0 needed for the same change of the linear relaxation function at T_a . The opposite applies for a down jump. In both cases Eq. (4) provides the SPA recipe for calculating $R_{\text{lin}}(t)$ from nonlinear jump data in the form of $R(t)$. This is done in a step-by-step manner starting at $t = 0$ [36, 37, 46]. Since $R_{\text{lin}}(t)$ for all jumps to T_a must be the same function, the material-characteristic nonlinearity parameter c can be determined by optimizing the collapse of the $R_{\text{lin}}(t)$ functions calculated from different temperature jumps.

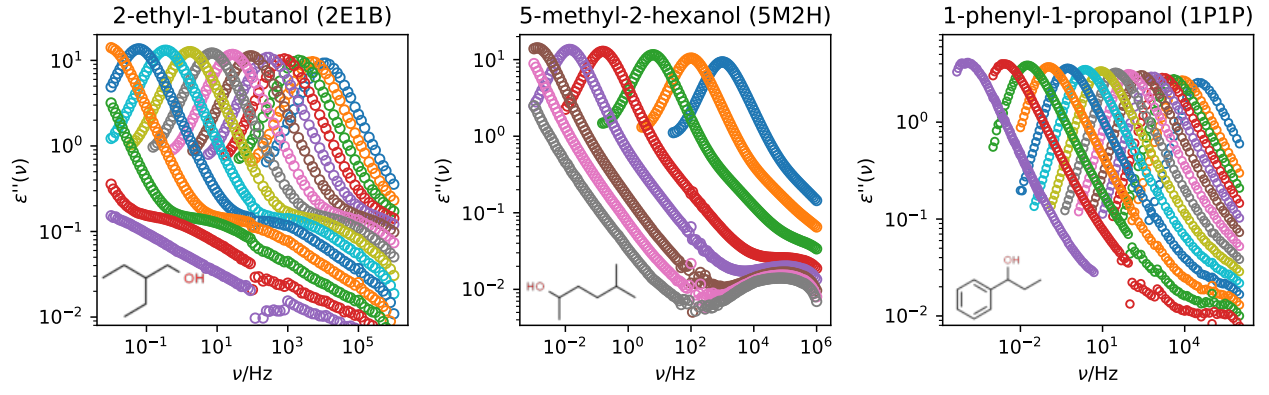


FIG. 1. Equilibrium dielectric spectra at different temperatures of 2E1B, 5M2H, and 1P1P. The figure shows the imaginary part of the frequency-dependent dielectric constant ϵ'' as a function of the frequency ν plotted in a log-log plot. The insets show the molecular structures.

III. RESULTS AND DISCUSSION

2E1B [K]	5M2H [K]	1P1P [K]
200	193	230
195	183	225
190	173	222.5
185	163	220
180	158	217.5
175	154	215
170	152	212.5
165	150	210
160		207.5
155		205
150		202.5
145		200
140		197.5
135		195
130		193

TABLE I. Temperatures for the equilibrium dielectric spectra of Fig. 1.

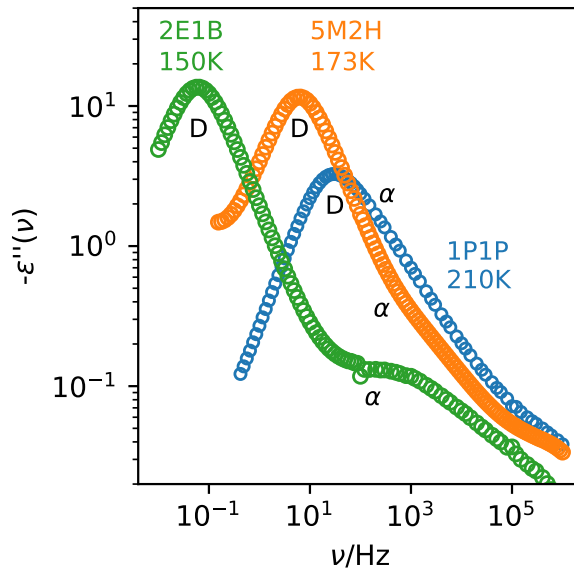


FIG. 2. Examples of dielectric loss peaks of 2E1B (green), 5M2H (orange), and 1P1P (blue). The Debye peak is marked by the letter D and the α peak by an α . For 2E1B the latter is clearly visible, while it for 5M2H is manifested as a change of slope. In contrast, the 1P1P loss peak is asymmetric and looks much like those of typical non-monoalcohol organic glass formers [52, 53]. Even for 1P1P, however, supplementary dynamic light scattering measurements revealed the existence of separate Debye and α peaks, albeit close to each other [38, 54].

Figure 1 shows equilibrium dielectric loss spectra of the three monoalcohols for a range of temperatures. To compare the liquids we plot in Fig. 2 three representative loss spectra. 2E1B and 5M2H have large, symmetric, narrow loss peaks. These are the noted Debye loss peaks (marked by D), the above-discussed characteristic feature of monoalcohols [38]. For 2E1B there is clearly an additional high-frequency process; this is identified as the α process [38]. An underlying α process is also visible in the 5M2H data, though it is much less pronounced and merely visible as a change of slope. The 1P1P loss peak, on the other hand, has no clearly visible Debye process. Its peak is broader and asymmetric to the high-frequency side with a high-frequency slope that is not far from -0.5 [52, 53]; thus the 1P1P loss peak looks like typical peaks of van der Waals bonded liquids [26, 52]. If there is a dielectric Debye process in 1P1P, it has merged completely with the α process. However, a closer analysis involving also light-scattering data that are known to mainly probe the self part of the dipole time-autocorrelation function [53], reveals that the dielectric spectrum of 1P1P may also be perceived as a sum of a Debye and an α peak [38, 54].

The aging data and their subsequent analysis are presented in Fig. 3. The top three panels show all temperature jump data. Data are the imaginary part of the dielectric permittivity measured at a fixed frequency (1kHz for 5M2H and 10kHz for 2E1B and 1P1P), plotted as a function of the logarithm of the time after the jump was initiated. For 2E1B there are jumps to two final temperatures, for 5M2H to five final temperatures, and for 1P1P to three final temperatures. The jump magnitudes vary from 0.1 K to 2.9 K (Table II).

Using $X = \varepsilon''(\nu_0, t)$, where $\nu_0 = 1$ kHz or 10 kHz, as the monitored variable, the second row of Fig. 3 shows all the corresponding normalized relaxation functions $R(t)$, defined by Eq. (1), plotted as functions of time. Note that the normalized relaxation functions do not start in unity at short times; this is because there is a rapid change of the dielectric loss, which is too fast to be probed by the setup. The functions $R(t)$ do not collapse, even for jumps to the same temperature (same color). This illustrates the above-mentioned strong nonlinearity of physical aging [7]. In order to arrive at the linear-limit normalized relaxation function, $R_{\text{lin}}(t)$, we employ single-parameter aging (SPA) as detailed in Sec. II B. The fitting procedure involves just a single free parameter for each liquid, the “nonlinearity parameter” c in Eq. (2). SPA uniquely determines $R_{\text{lin}}(t)$ from the normalized relaxation function of any jump, $R(t)$. For each liquid, c is found by searching for the best overall collapse of all calculated linear-limit aging curves. This results in $c = 1.72 \text{ K}^{-1}$ for 2E1B and $c = 1.19 \text{ K}^{-1}$ for both 5M2H and 1P1P.

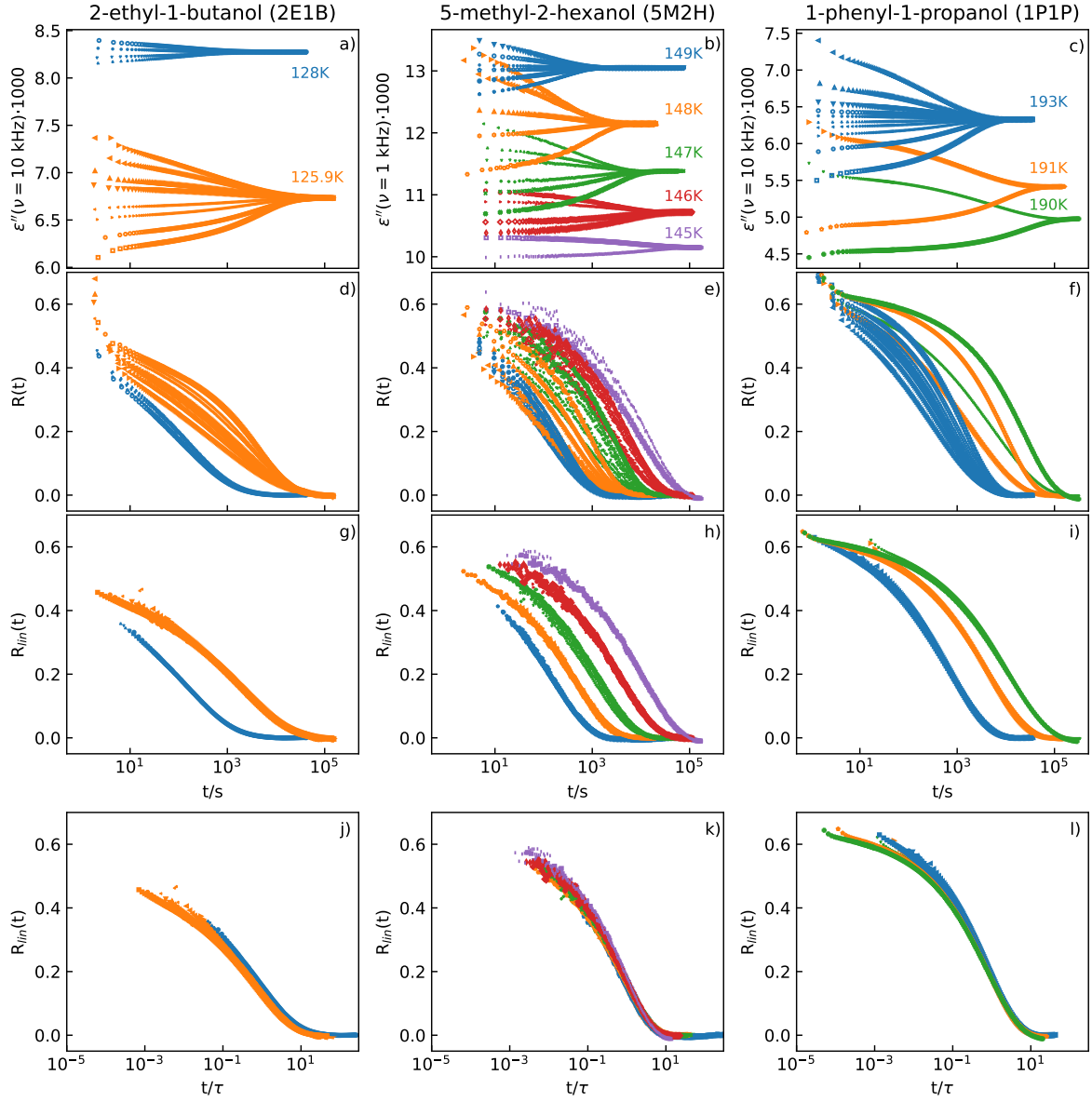


FIG. 3. Aging data and SPA analysis. The left panels show data for 2E1B, the middle panels for 5M2H, the right panels for 1P1P. (a)-(c) show data for the imaginary part of the dielectric susceptibility measured at the indicated frequency after a temperature jump at $t = 0$. (d)-(f) show the normalized relaxation functions corresponding to the data of (a)-(c) defined by Eq. (1) using as monitored property, X , the imaginary dielectric susceptibility. (g)-(i) show for each final temperature collapse of the different jump data when these are transformed into a linear aging relaxation function by means of Eq. (4). The transformation involves a single substance-specific parameter, c , which for each liquid is determined by best data collapse. (j)-(l) collapse the linear aging relaxation function for different target temperatures to a single one by empirically rescaling the time axis. The data collapse seen here confirms time-temperature superposition, which is a prerequisite of the TN formalism and therefore also for SPA.

2E1B			5M2H			1P1P		
T_i/K	T_a/K	$\Delta T/K$	T_i/K	T_a/K	$\Delta T/K$	T_i/K	T_a/K	$\Delta T/K$
127.8	128	0.2	148.9	149	0.1	192.9	193	0.1
127.5	128	0.5	148.5	149	0.5	192.75	193	0.25
125.4	125.9	0.5	148	149	1.0	192.5	193	0.5
125	125.9	0.9	147.5	148	0.5	192	193	1.0
124.1	125.9	1.8	146.1	148	1.9	191	193	2.0
123.2	125.9	2.7	145.1	148	2.9	189	191	2.0
127.8	128	0.2	146.5	147	0.5	188	190	2.00
128.5	128	-0.5	146	147	1.0	193.1	193	-0.1
126	125.9	-0.1	145.1	147	1.9	193.25	193	-0.25
126.4	125.9	-0.5	145.5	146	0.5	193.5	193	-0.5
126.8	125.9	-0.9	145	146	1.0	194	193	-1.0
127.8	125.9	-1.9	144.5	145	0.5	195	193	-2.0
			149.1	149	-0.1	193	191	2.00
			149.5	149	-0.5	192	190	2.00
			150	149	-1.0			
			148.5	148	-0.5			
			149.9	148	-1.9			
			147.5	147	-0.5			
			148	147	-1.0			
			148.9	147	-1.9			
			146.5	146	-0.5			
			147	146	-1.0			
			145.5	145	-0.5			

TABLE II. List of all temperature jumps performed, starting from the initial temperature T_i and going to the final (annealing) temperature T_a . The jump magnitudes $\Delta T \equiv T_a - T_i$ are also listed.

The obtained linear-limit normalized relaxation functions, $R_{\text{lin}}(t)$, are shown in the third row of Fig. 3. There is a good data collapse, which validates SPA. In the fourth row we empirically scale the time axis, which for all three liquids results in a good overall data collapse. This provides a further consistency check of the analysis, because the TN formalism – and thus SPA – assumes time-temperature superposition for the linear normalized relaxation functions.

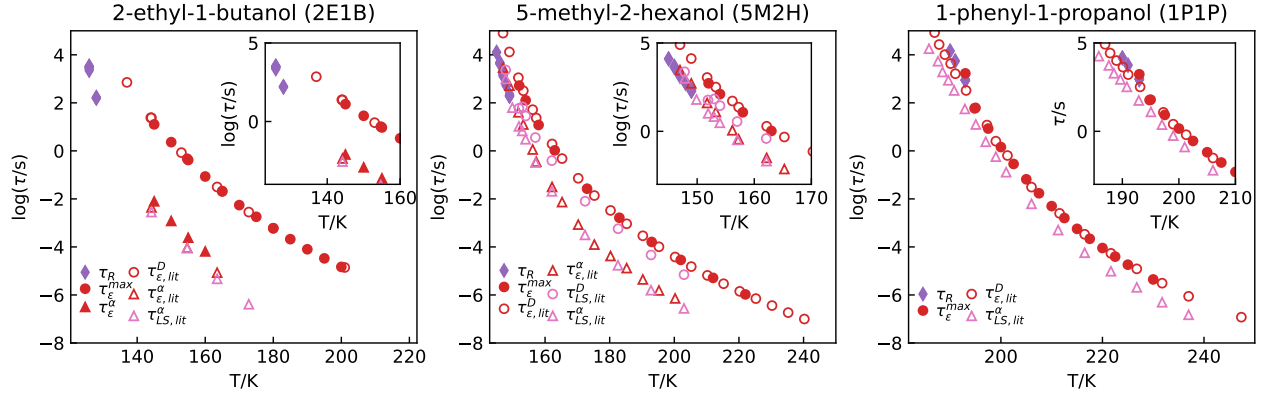


FIG. 4. Characteristic times τ plotted as functions of temperature for the three monoalcohols, including here also light-scattering data. The full symbols are defined as follows (compare the lower left corners that give the corresponding symbols): τ_R is the linear-limit aging time calculated as one over the loss-peak angular frequency of the Laplace transform of $R_{\text{lin}}(t)$ determined from the nonlinear aging data by SPA via Eq. (2) (though hardly visible, the figure reports one point for each temperature jump); $\tau_\epsilon^{\text{max}}$ is the inverse dielectric loss-peak angular frequency; τ_ϵ^α is the dielectric α relaxation time estimated as the inverse dielectric loss-peak angular frequency (by visual inspection); the open symbols are data from the literature [55–58]. For 2E1B and 5M2H the linear aging times follow the α times, not the Debye times, in their values and temperature dependencies. For 1P1P, which is characterized by an almost complete merging of the dielectric Debye and α processes (Fig. 2), it would be premature to conclude although the data point to the linear-limit aging times following the Debye times better than the α times.

From the functions $R_{\text{lin}}(t)$ we extract the linear-limit aging relaxation time at each final temperature as the inverse

of the loss-peak angular frequency of the Laplace transform of $R_{\text{lin}}(t)$. Having done so, we can now address this paper's scientific question: Does the temperature dependence of the linear aging time, τ_R , follow that of the α process – as most other physical processes do [38, 43, 44] – or does it follow the slower Debye process [59–61]? To answer this we plot for each liquid in Fig. 4 as functions of temperature: the Debye relaxation times [55–58], the α process relaxation times extracted by dielectric spectroscopy [55–58], and the dynamic-light-scattering relaxation times [56–58].

In general, different linear-response functions may have different characteristic relaxation times [41–44], i.e., the same underlying process can have different relaxation times when observed with different techniques. A trivial example of this is the comparison of the compliance and modulus representation of the same data: depending on the relaxation strength, this can lead to very different relaxation times. For several liquids, a time-scale ordering has been established, where the thermal response functions, i.e., response functions where the input is a temperature modulation (dynamic heat capacity, thermal expansion coefficient, etc) – are slower than the dielectric response functions by up to one decade [43, 44]. This means that it is not possible to reach a conclusion by comparing time scales alone (although they usually do not differ by more than a decade). Thus in order to determine whether physical aging follows the Debye or the α process, we must not only take into account the proximity of the relaxation times but also how the corresponding relaxation times vary with temperature.

The aging data cover a smaller temperature range than the other data of Fig. 4. The figure nevertheless illuminates the physics of aging and its relation to dielectric processes. For the two monoalcohols with the most pronounced and clearly separated Debye processes, 2E1B and 5M2H, the conclusion is clear: Physical aging follows the α process, not the Debye process. For 2E1B there is no overlap between the α relaxation times extracted from the dielectric spectra and the aging relaxation time, but the separation between the Debye time scale and the aging relaxation time clearly exceeds 2-3 decades and the aging time follows the temperature dependence of the dielectric α relaxation time rather than of the dielectric Debye relaxation time. In the case of 5M2H, the α relaxation time found by dielectrics and light scattering is identical to the linear aging relaxation time: In this case both time scale and temperature dependence match. For 1P1P the picture is less clear. Here a separate α and Debye processes have been determined from data for non-linear dielectric spectroscopy [62] and light scattering [63]. While these data appear to indicate that aging follows the Debye and not the α process, we hesitate to conclude this firmly, because the α and the Debye dielectric processes of 1P1P are so close that the time scale separation in itself is inconclusive. In addition, the processes are merged to such an extent that they cannot be distinguished visually at any temperature, which also means that the temperature dependence of the two processes for all practical purposes is identical.

The fact that the Debye process in 2E1B and 5M2H appears to have no relation to the linear aging timescale, while the situation is different for 1P1P, suggests a different underlying origin of the cross-correlations responsible for the Debye process. In other words, our results point to the possible existence of different classes of Debye processes: In some systems the linear aging time scale clearly follows the dielectric α relaxation, in other systems it is closer the dielectric Debye process. Such a difference makes sense in view of the fact that hydrogen structures evolve very differently in different systems in the form of chains [64], rings [64, 65], or in a branched [66] form. Thus 2E1B and 2E1H are classical chain-like alcohols, while 1P1P is believed to form a mixture of ring- and chain-like structures. Note also that additional cross-correlations can form in phenyl alcohols due to the pi-pi electron systems [67, 68], as has also been observed in recent simulations [69].

Only few other investigations have compared aging times to other relaxation times. Gainaru *et al.* found indications that the dielectric aging of 2-ethyl-1-hexanol (2E1H) and 2-ethyl-1-hexyl bromide follows the α process [59], while in the non-hydrogen-bonding liquid tri-butyl-phosphate (TBP) with an alcohol-like spectrum created by dielectric cross-correlation, the linear aging time follows the Debye-like mode associated with dielectric cross-correlations [60, 61].

IV. SUMMARY

We have presented data for the physical aging of three monoalcohols obtained by monitoring the high-frequency dielectric loss after up and down temperature jumps of small and moderate magnitude. The aging of all three liquids conforms to SPA, which allows one to extract the linear-limit normalized aging relaxation functions $R_{\text{lin}}(t)$ at each final temperature. From these functions, we determined the linear-limit aging relaxation times as the inverse of the loss-peak angular frequencies of the Laplace transform of $R_{\text{lin}}(t)$. Comparing to the temperature dependence of the Debye and α relaxation inverse loss peak frequencies, the analysis showed that for the two liquids with best separation of the Debye and the α processes, 2E1B and 5M2H, physical aging follows the α process and not the Debye process. The third liquid, 1P1P, appears to follow the Debye process in its aging-time temperature dependence, but no definite conclusion can be made at this point because the Debye and α relaxation times are quite close for this system.

ACKNOWLEDGMENTS

This work was supported by the VILLUM Foundation's *Matter* grant (VIL16515).

-
- [1] F. Simon, Über den Zustand der unterkühlten Flüssigkeiten und Gläser, *Z. Anorg. Allg. Chem.* **203**, 219 (1931).
- [2] W. Kauzmann, The nature of the glassy state and the behavior of liquids at low temperatures, *Chem. Rev.* **43**, 219 (1948).
- [3] O. S. Narayanaswamy, A model of structural relaxation in glass, *J. Amer. Ceram. Soc.* **54**, 491 (1971).
- [4] O. Mazurin, Relaxation phenomena in glass, *J. Non-Cryst. Solids* **25**, 129 (1977).
- [5] L. C. E. Struik, *Physical Aging in Amorphous Polymers and Other Materials* (Elsevier, Amsterdam, 1978).
- [6] A. J. Kovacs, J. J. Aklonis, J. M. Hutchinson, and A. R. Ramos, Isobaric volume and enthalpy recovery of glasses. II. A transparent multiparameter theory, *J. Polym. Sci. Polym. Phys.* **17**, 1097 (1979).
- [7] G. W. Scherer, *Relaxation in Glass and Composites* (Wiley, New York, 1986).
- [8] I. M. Hodge, Physical aging in polymer glasses, *Science* **267**, 1945 (1995).
- [9] L. Grassia and S. L. Simon, Modeling volume relaxation of amorphous polymers: Modification of the equation for the relaxation time in the KAHR model, *Polymer* **53**, 3613 (2012).
- [10] D. Cangialosi, V. M. Boucher, A. Alegria, and J. Colmenero, Physical aging in polymers and polymer nanocomposites: recent results and open questions, *Soft Matter* **9**, 8619 (2013).
- [11] M. Micoulaut, Relaxation and physical aging in network glasses: a review, *Rep. Prog. Phys.* **79**, 066504 (2016).
- [12] G. B. McKenna and S. L. Simon, 50th anniversary perspective: Challenges in the dynamics and kinetics of glass-forming polymers, *Macromolecules* **50**, 6333 (2017).
- [13] C. B. Roth, ed., *Polymer Glasses* (CRC Press (Boca Raton, FL, USA), 2017).
- [14] B. Ruta, E. Pineda, and Z. Evenson, Relaxation processes and physical aging in metallic glasses, *J. Phys.: Condens. Matter* **29**, 503002 (2017).
- [15] J. C. Mauro, *Materials Kinetics: Transport and Rate Phenomena* (Elsevier, Amsterdam, Netherlands, 2021).
- [16] A. Q. Tool, Relation between inelastic deformability and thermal expansion of glass in its annealing range, *J. Amer. Ceram. Soc.* **29**, 240 (1946).
- [17] A. J. Kovacs, Transition vitreuse dans les polymeres amorphes. Etude phenomenologique, *Fortschr. Hochpolym.-Forsch.* **3**, 394 (1963).
- [18] C. T. Moynihan, P. B. Macedo, C. J. Montrose, P. K. Gupta, M. A. DeBolt, J. F. Dill, B. E. Dom, P. W. Drake, A. J. Easteal, P. B. Elterman, R. P. Moeller, H. Sasabe, and J. A. Wilder, Structural relaxation in vitreous materials, *Ann. NY Acad. Sci.* **279**, 15 (1976).
- [19] H. S. Chen, The influence of structural relaxation on the density and Young's modulus of metallic glasses, *J. Appl. Phys.* **49**, 3289 (1978).
- [20] N. B. Olsen, J. C. Dyre, and T. Christensen, Structural relaxation monitored by instantaneous shear modulus, *Phys. Rev. Lett.* **81**, 1031 (1998).
- [21] J. C. Dyre and N. B. Olsen, Minimal model for beta relaxation in viscous liquids, *Phys. Rev. Lett.* **91**, 155703 (2003).
- [22] R. Di Leonardo, T. Scopigno, G. Ruocco, and U. Buontempo, Spectroscopic cell for fast pressure jumps across the glass transition line, *Rev. Sci. Instrum.* **75**, 2631 (2004).
- [23] E. Schlosser and A. Schönhals, Dielectric relaxation during physical aging, *Polymer* **32**, 2135 (1991).
- [24] P. Lunkenheimer, R. Wehn, U. Schneider, and A. Loidl, Glassy aging dynamics, *Phys. Rev. Lett.* **95**, 055702 (2005).
- [25] C. Brun, F. Ladieu, D. L'Hôte, G. Biroli, and J.-P. Bouchaud, Evidence of growing spatial correlations during the aging of glassy glycerol, *Phys. Rev. Lett.* **109**, 175702 (2012).
- [26] R. Richert, Supercooled liquids and glasses by dielectric relaxation spectroscopy, *Adv. Chem. Phys.* **156**, 101 (2015).
- [27] V. Di Lisio, L. A. Rocchi, and D. Cangialosi, Twofold facet of kinetics of glass aging, *Phys. Rev. Lett.* **133**, 048201 (2024).
- [28] P. K. Bera, G. A. Medvedev, J. M. Caruthers, and M. D. Ediger, Structural relaxation time of a polymer glass during deformation, *Phys. Rev. Lett.* **132**, 208101 (2024).
- [29] B. Igarashi, T. Christensen, E. H. Larsen, N. B. Olsen, I. H. Pedersen, T. Rasmussen, and J. C. Dyre, A cryostat and temperature control system optimized for measuring relaxations of glass-forming liquids, *Rev. Sci. Instrum.* **79**, 045105 (2008).
- [30] M. Hénot and F. Ladieu, Non-linear physical aging of supercooled glycerol induced by large upward ideal temperature steps monitored through cooling experiments, *J. Chem. Phys.* **158**, 224504 (2023).
- [31] V. Di Lisio, V.-M. Stavropoulou, and D. Cangialosi, Physical aging in molecular glasses beyond the α relaxation, *J. Chem. Phys.* **159**, 064505 (2023).
- [32] V. Di Lisio, L. A. Rocchi, and D. Cangialosi, Twofold facet of kinetics of glass aging, *Phys. Rev. Lett.* **133**, 048201 (2024).
- [33] J. C. Mauro, P. K. Gupta, and R. J. Loucks, Composition dependence of glass transition temperature and fragility. ii. a topological model of alkali borate liquids, *J. Chem. Phys.* **130**, 234503 (2009).
- [34] J. K. Nielsen and J. C. Dyre, Fluctuation-dissipation theorem for frequency-dependent specific heat, *Phys. Rev. B* **54**, 15754 (1996).
- [35] K. Niss, J. C. Dyre, and T. Hecksher, Long-time structural relaxation of glass-forming liquids: Simple or stretched exponential?, *J. Chem. Phys.* **152**, 041103 (2020).

- [36] B. Riechers, L. A. Roed, S. Mehri, T. S. Ingebrigtsen, T. Hecksher, J. C. Dyre, and K. Niss, Predicting nonlinear physical aging of glasses from equilibrium relaxation via the material time, *Sci. Adv.* **8**, eabl9809 (2022).
- [37] T. Hecksher, N. B. Olsen, and J. C. Dyre, Communication: Direct tests of single-parameter aging, *J. Chem. Phys.* **142**, 241103 (2015).
- [38] R. Böhmer, C. Gainaru, and R. Richert, Structure and dynamics of monohydroxy alcohols – Milestones towards their microscopic understanding, 100 years after Debye, *Phys. Rep.* **545**, 125 (2014).
- [39] H. Huth, L.-M. Wang, C. Schick, and R. Richert, Comparing calorimetric and dielectric polarization modes in viscous 2-ethyl-1-hexanol, *The Journal of chemical physics* **126** (2007).
- [40] L.-M. Wang, Y. Tian, R. Liu, and R. Richert, Calorimetric versus kinetic glass transitions in viscous monohydroxy alcohols, *The Journal of chemical physics* **128** (2008).
- [41] M. Cutroni and A. Mandanici, The α -relaxation process in simple glass forming liquid m-toluidine. ii. the temperature dependence of the mechanical response, *Journal of Chemical Physics* **114**, 7124 (2001), https://pubs.aip.org/aip/jcp/article-pdf/114/16/7124/19137151/7124_1_online.pdf.
- [42] B. Jakobsen, K. Niss, and N. B. Olsen, Dielectric and shear mechanical alpha and beta relaxations in seven glass-forming liquids, *The Journal of Chemical Physics* **123**, 234511 (2005), https://pubs.aip.org/aip/jcp/article-pdf/doi/10.1063/1.2136887/15374828/234511_1_online.pdf.
- [43] B. Jakobsen, T. Hecksher, T. Christensen, N. B. Olsen, J. C. Dyre, and K. Niss, Communication: Identical temperature dependence of the time scales of several linear-response functions of two glass-forming liquids, *The Journal of Chemical Physics* **136** (2012).
- [44] L. A. Roed, J. C. Dyre, K. Niss, T. Hecksher, and B. Riechers, Time-scale ordering in hydrogen- and van der Waals-bonded liquids, *J. Chem. Phys.* **154**, 184508 (2021).
- [45] K. Niss, Mapping isobaric aging onto the equilibrium phase diagram, *Phys. Rev. Lett.* **119**, 115703 (2017).
- [46] L. A. Roed, T. Hecksher, J. C. Dyre, and K. Niss, Generalized single-parameter aging tests and their application to glycerol, *J. Chem. Phys.* **150**, 044501 (2019).
- [47] S. Mehri, T. S. Ingebrigtsen, and J. C. Dyre, Single-parameter aging in a binary Lennard-Jones system, *J. Chem. Phys.* **154**, 094504 (2021).
- [48] T. Böhmer, J. P. Gabriel, L. Costigliola, J.-N. Kociok, T. Hecksher, J. C. Dyre, and T. Blochowicz, Time reversibility during the ageing of materials, *Nat. Phys.* **20**, 637 (2024).
- [49] M. Henot, X. A. Nguyen, and F. Ladieu, Crossing the frontier of validity of the material time approach in the aging of a molecular glass, *J. Phys. Chem. Lett.* **15**, 3170 (2024).
- [50] T. Hecksher and K. Niss, Single parameter aging and density scaling, *Journal of Chemical Physics* **161**, 194504 (2024), https://pubs.aip.org/aip/jcp/article-pdf/doi/10.1063/5.0234620/20260339/194504_1_5.0234620.pdf.
- [51] T. Hecksher, N. B. Olsen, and J. C. Dyre, Fast contribution to the activation energy of a glass-forming liquid, *Proc. Natl. Acad. Sci. (USA)* **116**, 16736 (2019).
- [52] A. I. Nielsen, T. Christensen, B. Jakobsen, K. Niss, N. B. Olsen, R. Richert, and J. C. Dyre, Prevalence of approximate \sqrt{t} relaxation for the dielectric α process in viscous organic liquids, *J. Chem. Phys.* **130**, 154508 (2009).
- [53] F. Pabst, J. P. Gabriel, T. Böhmer, P. Weigl, A. Helbling, T. Richter, P. Zourchang, T. Walther, and T. Blochowicz, Generic structural relaxation in supercooled liquids, *J. Phys. Chem. Lett.* **12**, 3685 (2021).
- [54] C. Hansen, F. Stickel, T. Berger, R. Richert, and E. W. Fischer, Dynamics of glass-forming liquids. iii. comparing the dielectric α - and β -relaxation of 1-propanol and o-terphenyl, *The Journal of chemical physics* **107**, 1086 (1997).
- [55] S. Bauer, K. Burlafinger, C. Gainaru, P. Lunkenheimer, W. Hiller, A. Loidl, and R. Böhmer, Debye relaxation and 250 k anomaly in glass forming monohydroxy alcohols, *The Journal of chemical physics* **138** (2013).
- [56] J. Gabriel, F. Pabst, A. Helbling, T. Böhmer, and T. Blochowicz, Nature of the debye-process in monohydroxy alcohols: 5-methyl-2-hexanol investigated by depolarized light scattering and dielectric spectroscopy, *Phys. Rev. Lett.* **121**, 035501 (2018).
- [57] J. Gabriel, F. Pabst, A. Helbling, T. Böhmer, and T. Blochowicz, Depolarized dynamic light scattering and dielectric spectroscopy: Two perspectives on molecular reorientation in supercooled liquids, in *The Scaling of Relaxation Processes*, edited by F. Kremer and A. Loidl (Springer International Publishing, 2018) pp. 203–245.
- [58] J. Gabriel, *Depolarisierte Dynamische Lichtstreuung an Monohydroxy-Alkoholen*, Ph.D. thesis, Technische Universität (2018).
- [59] C. Gainaru and R. Böhmer, Coupling of the electrical conductivity to the structural relaxation, absence of physical aging on the time scale of the debye process, and number of correlated molecules in the supercooled monohydroxy alcohol 2-ethylhexanol, *Journal of non-crystalline solids* **356**, 542 (2010).
- [60] K. Moch, P. Münzner, R. Böhmer, and C. Gainaru, Molecular cross-correlations govern structural rearrangements in a nonassociating polar glass former, *Physical Review Letters* **128**, 228001 (2022).
- [61] J. P. Gabriel and R. Richert, Comparing two sources of physical aging: Temperature vs electric field, *The Journal of Chemical Physics* **159** (2023).
- [62] J. P. Gabriel, E. Thoms, and R. Richert, High electric fields elucidate the hydrogen-bonded structures in 1-phenyl-1-propanol, *Journal of Molecular Liquids* **330**, 115626 (2021).
- [63] T. Böhmer, J. P. Gabriel, T. Richter, F. Pabst, and T. Blochowicz, Influence of molecular architecture on the dynamics of h-bonded supramolecular structures in phenyl-propanols, *The Journal of Physical Chemistry B* **123**, 10959 (2019).
- [64] G. P. Johari and W. Dannhauser, Dielectric study of intermolecular association in sterically hindered octanol isomers, *J. Phys. Chem.* **72**, 3273 (1968).

- [65] L. P. Singh and R. Richert, Watching hydrogen-bonded structures in an alcohol convert from rings to chains, *Phys. Rev. Lett.* **109**, 10.1103/PhysRevLett.109.167802 (2012).
- [66] P. Sillrén, J. Bielecki, J. Mattsson, L. Borjesson, and A. Matic, A statistical model of hydrogen bond networks in liquid alcohols, *J. Chem. Phys.* **136**, 10.1063/1.3690137 (2012).
- [67] A. Nowok, K. Jurkiewicz, M. Dulski, H. Hellwig, J. G. Małecki, K. Grzybowska, J. Grelka, and S. Pawlus, Influence of molecular geometry on the formation, architecture and dynamics of h-bonded supramolecular associates in 1-phenyl alcohols, *Journal of Molecular Liquids* **326**, 115349 (2021).
- [68] A. Nowok, M. Dulski, K. Jurkiewicz, J. Grelka, A. Z. Szeremeta, K. Grzybowska, and S. Pawlus, Molecular stiffness and aromatic ring position–crucial structural factors in the self-assembly processes of phenyl alcohols, *Journal of Molecular Liquids* **335**, 116426 (2021).
- [69] J. Grelka, K. Jurkiewicz, A. Nowok, and S. Pawlus, Computer simulations as an effective way to distinguish supramolecular nanostructure in cyclic and phenyl alcohols, *Physical Review E* **108**, 024603 (2023).